Biochimica et Biophysica Acta, 682 (1982) 322–331
Elsevier Biomedical Press

BBA 41193

LOW-INTENSITY PICOSECOND FLUORESCENCE KINETICS AND EXCITATION DYNAMICS IN BARLEY CHLOROPLASTS

ROBERT J. GULOTTY [a], GRAHAM R. FLEMING [a] and RANDALL S. ALBERTE [b]

Departments of Chemistry [a] and Biology [b], The University of Chicago, 5735 South Ellis Avenue, Chicago, IL 60637 (U.S.A.)

(Received March 24th, 1982)
(Revised manuscript received August 4th, 1982)

Key words: Fluorescence decay; Photon counting; Excitation transfer; (Barley chloroplast)

The fluorescence decays of barley chloroplasts have been measured by single-photon counting with tunable picosecond dye laser excitation. The fluorescence decays of dark-adapted chloroplasts are best fitted to a sum of three exponential lifetime components with 1/e lifetimes of 112, 380 and 2214 ps. The relative magnitude of each component is shown to be dependent on the excitation wavelength and collected emission wavelength. The excitation wavelength dependence is correlated with the Photosystem (PS) I and PS II action study of Ried [36] and with the measured pigment distributions in the photosynthetic unit [37,41]. Experiments varying the single excitation pulse intensity from 10^8 to 10^{12} photons/cm^2 pulse show that our results are not distorted by singlet-singlet annihilation. Unflowed samples where the cloroplasts are under constant illumination show 2-fold increases in quantum yield of fluorescence primarily in the two longer 1/e lifetime components. Theoretical calculations of Shipman [31] on an isolated reaction center with a homogeneous antenna are discussed and the principles extended to discussion of the measured barley chloroplast fluorescence decay components in terms of photosynthetic unit light-harvesting array models and earlier experimental work. Our data support a photosynthetic unit model in which 70–90% of the photons absorbed are quenched by either PS I or efficiently quenching PS II in a process where the fluorescence lifetime is 100 ps. The origin of the intermediate 380 ps component is probably due to excitation transfer to a PS II reaction center in a redox state which quenches less efficiently.

Introduction

The analysis of the fluorescence decay of excitation in the light-harvesting system of chloroplasts has the potential to provide valuable information on the mechanism of energy transfer to the reaction centers and on the organization of the light-harvesting system. To date, steady-state fluorescence and fluorescence quantum yield measurements have been the major methods used to probe the structural organization and energy-transfer properties in and among photosynthetic units. However, for an inhomogeneous collection of chlorophylls associated with distinct proteins and reaction centers in the chloroplast, which emit at approximately the same maximum wavelength at physiological temperatures, there is no unambiguous way to infer specific rate processes or energy-transfer mechanisms and paths from steady-state quantum yields. Newly developed time-resolved fluorescence techniques, though, are capable of providing important information regarding the origins of the fluorescence in terms of structural areas in the photosynthetic unit, and the physical

Abbreviations: Chl, chlorophyll; PS, photosystem; Hepes; *N*-2-hydroxyethylpiperazine-*N'*-2-ethanesulfonic acid.

0005-2728/82/0000–0000/$02.75

mechanism and phenomenological paths of energy transfer.

While the potential of time-resolved kinetic measurements in providing information regarding the mechanism of energy transfer and structural organization in the photosynthetic light-harvesting system is great, there are a number of experimental and theoretical limitations to attaining this potential. The theoretical limitations involve the number of decay channels and heterogeneity of the light-harvesting system in chloroplasts. Experimentally, it is difficult to resolve complex functional decay forms, and to avoid artifacts which could arise from the measurement of picosecond photophysical events in photochemically sensitive systems.

Three basic approaches to the measurements of fluorescence decays have been used. Barber and co-workers [1,2], Campillo and co-workers [3,4], Yu et al. [5] and Paschenko et al. [6] have used single pulses from mode-locked solid-state lasers for excitation and streak camera detection. This method has the advantage of good time resolution, and the disadvantages of relatively low dynamic range, low signal-to-noise ratio and high-intensity excitation [7,8]. In addition, few wavelenghts were available, and the majority of this work has used 530 nm excitation where carotenoids absorb strongly and chlorophyll weakly. The second technique, the phase-shift method, has been used by Borisov and Il'ina [9,10] for studies of both green plants and photosynthetic bacteria. Although, in principle, multiexponential decays can be resolved with this technique [11], only average lifetimes have been obtained for photosynthetic systems to date. The third technique, time-correlated single-photon counting, has been used by Beddard and co-workers [12] and Sauer and co-workers [13–15]. The time resolution of this technique is less than that of the streak camera, however, and the dynamic range and signal-to-noise ratio are very high ($1 \cdot 10^5 : 1$ dynamic range). Further, in combination with a tunable synchronously pumped picosecond dye laser, it is possible to use very weak excitation pulses at any wavelength in the visible to near-infrared spectral region. These advantages recommend the photon-counting technique in spite of the possible complications which could arise from the high repetition rate of the synchronously mode-locked laser.

In the present study, we employed the synchronously pumped dye laser photon-counting method to examine the picosecond fluorescence decay kinetics and excitation dynamics of barley chloroplasts. The large dynamic range of this technique was critical to the fitting of the complex fluorescence decays, while the ability to vary excitation wavelength and the possibility of exciting specific groups of pigment molecules added a new dimension to the studies. In addition, recent improvements in the time resolution of the photon-counting system in the red spectral region (650–850 nm) by about a factor of three over the previous best resolution [12] provide us with a time resolution of less than 50 ps.

In this work is described what is believed to be the most thorough determination of the fluorescence decay of intact chloroplasts. It is found that these decays are best fitted to a sum of three single-exponential decay functions. Meaning is assigned to the fluorescence decay components by varying the excitation wavelength from 600 to 700 nm, the emission wavelength from 665 to 730 nm, and the state of the reaction centers by preillumination.

Materials and Methods

Chloroplasts of greenhouse-grown wild-type barley (*Hordeum vulgare*) and store-bought spinach (*Spinacea oleracea*) were isolated according to the method of Mills and Joy [16]. The chloroplasts were suspended in 1 l of low-salt buffer (0.33 M sorbitol, 10 mM Hepes) and adjusted to pH 7.6 with NaOH. The samples were kept on ice throughout the isolation and were maintained at 5–10°C for the fluorescence decay measurements. Other isolation techniques were employed for comparison [15,17,18] and found to yield chloroplasts which gave similar decay curves but lower percentages of class A chloroplasts [19]. Chloroplast intactness was checked by $Fe(CN)_6^{3-}$-dependent oxygen evolution in a Clark-type oxygen electrode [20] and by routine examination using phase-contrast microscopy [21]. Typically, greater than 50% of the isolated chloroplasts were of the class A type.

Rhodamine 6G, rhodamine 640 and DCM [22] dyes (Exciton Corp.) were used in a Coherent

CR-599 dye laser synchronously pumped by a Coherent CR-6 argon ion laser (mode-locked on the 5145 Å line) to provide picosecond pulses (10–20 ps, full-width at half-maximum) throughout a 600–700 nm wavelength region. Individual light pulse intensities were typically less than $2 \cdot 10^{12}$ photons/cm^2 per pulse. Experiments varying the single-pulse intensity from 10^8 to 10^{12} photons/cm^2 per pulse gave identical decays; this ensures that singlet-singlet annihilation [23–25] does not distort our results. The laser repetition rate was reduced from 91 MHz (10 ns between pulses) to 45 kHz (22 μs) with a Coherent Model 28 Pockels cell between extinguishing polarizers. Contrast ratios of 200–1000 : 1 for selected versus rejected pulse areas were achieved depending on Pockels cell alignment and excitation wavelength. A second Pockels cell was used in series to improve the contrast ratio by a factor of 10–100 over the entire wavelength region for comparison with lower levels of preillumination.

A Texas Instruments TIED-56 silicon avalanche photodiode provided the start pulse for the time-to-amplitude converter. An Amperex PM 31000A red-sensitive photomultiplier tube in a refrigerated housing was used to detect fluorescent photons at right angles to the excitation beam. The arrival of a single photon (hence, high-intensity pulses are not necessary) selected from at least 100 laser pulses was recorded at the time-to-amplitude converter.

Schott red glass cut-off filters and Ditric Optics 3-plate and wide-band interference filters were used in collecting fluorescence. Scattered light was checked with an interference filter at the excitation wavelength with the collecting filters in place and increased laser intensities, or by attenuation of the incident laser beam before the chamber with the collection filters. An instrument response function was collected at a right angle using nondairy creamer in water of the same approximate absorbance as that of the chloroplasts in the flow cell.

Single-exponential fits of rose bengal in methanol [26] with $\tau = 534 \pm 10$ ps (1/e lifetime) or Oxazine 725 in methanol with $\tau = 860 \pm 40$ and reduced χ^2_R values of 1.0–1.1 were used as standards to check the system performance at each excitation wavelength. The reduced χ^2_R [27] is defined as:

$$\chi^2_R = \frac{1}{N-\nu} \sum_{I=1}^{N} \frac{[D(I)-C(I)]^2}{C(I)} \quad (1)$$

where N is the total number of data points (approx. 500), ν is equal to the number of parameters in our fitting functions, $D(I)$ is the measured number of fluorescence counts at each data point, and $C(I)$ is the corresponding number of counts calculated for each data point by iterative fitting.

Since the response of our system to photons scattered from a 10–20 ps incident light pulse is approx. 300 ps (full-width at half-maximum) (see Fig. 1) and we are interested in lifetimes as short as 50 ps, it is necessary to deconvolute the physical decay from the distorted decay recorded. A nonlinear least-squares fitting program was assembled to fit the data to either a sum of two or three exponentials by iterative convolution [28,29].

Results

The single-photon-counting fluorescence decays of dark-adapted barley chloroplasts are best fitted to a sum of three single-exponential decay functions,

$$[\text{Chl}^*](t) = A_1 \cdot \exp(-t/T_1) + A_2 \cdot \exp(-t/T_2) + A_3 \cdot \exp(-t/T_3) \quad (2)$$

where $A_1 = 0.788$, $T_1 = 112$ ps, $A_2 = 0.207$, $T_2 = 380$ ps, $A_3 = 0.007$, and $T_3 = 2214$ ps. Fig. 1a shows a typical fitted decay curve $D(t)$ and instrument response function $I(t)$. Fig. 1b shows a plot of residuals for this fit of the data to Eqn. 2. Each residual point is the normalized difference between the measured and fitted curve. These residuals should show no systematic deviation about zero for a properly fitted curve. While this is the case for the residuals of the triple-exponential fit (Fig. 1b), the residuals of a double- or single-exponential fit (Fig. 1c and d, respectively) show systematic deviation. The average reduced χ^2_R (Eqn. 1) for the triple-exponential fit to dark-adapted barley chloroplasts is approx. 1.2 (see Table I), which is within one standard deviation of the expected value of 1.0 for a properly fitted curve with Gaussian noise. However, the double- and

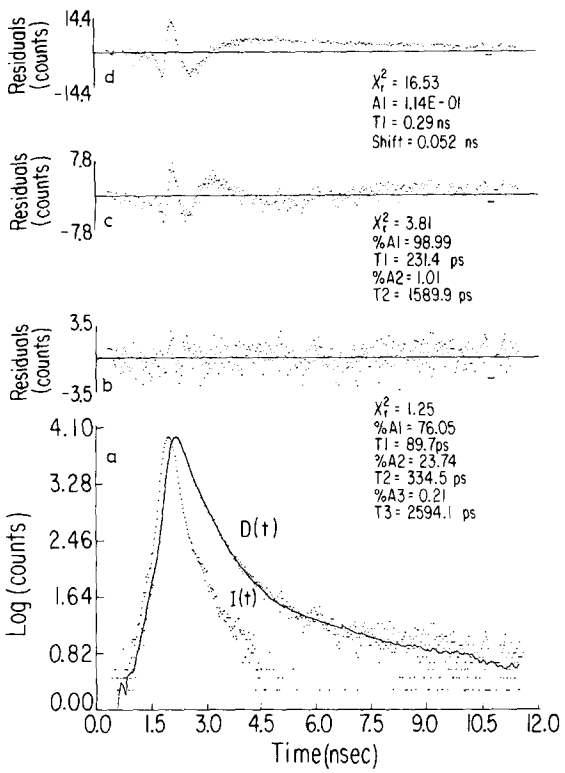

Fig. 1. (a) Fluorescence decay of dark-adapted barley chloroplasts excited at 600 ± 1 nm with fluorescence collected at 680 ± 10 nm. The curve and points labelled $D(t)$ show a triple-exponential fit (curve) to the measured fluorescence decay (points). The peak (points) labelled $I(t)$ is the instrument response function used in deconvoluting the molecular decay from the measured decay. (b) Residuals corresponding to the triple-exponential fit in part a. (c) Residuals for a double-exponential fit of the same fluorescence decay as in part a. (d) Residuals for a single-exponential fit to the fluorescence decay as in part a.

single-exponential fits typically show much higher reduced χ_R^2 values (e.g., Fig. 1c and d).

The parameters listed under Eqn. 2 and shown in Table I for the triple-exponential fit of dark-adapted barley chloroplasts are an average of 74 experimental decay curves. The excitation wavelength for these decays was varied from 600 to 700 nm in approx. 10-nm increments. The emission wavelength collected was varied from 680 to 730 nm in 10-nm increments using interference filters. In addition, all fluorescence wavelengths or long-wavelength fluorescence (i.e., greater than 665 or greater than 715 nm) were collected with cut-off filters.

The standard deviation values listed in Table I are much larger than the error of repeated measurement on a given sample under identical experimental conditions. The reason for this is that the averages in Table I were computed using data at all the different excitation and emission wavelengths used. Fig. 2 shows the way in which excitation wavelength causes the relative weights (preexponential factors in Eqn. 2 converted to percentages) of the three single-exponential decay terms to vary. The fluorescence was monitored with a 715 nm cut-off filter. There is a decrease in the relative percentage of the 112 ps lifetime component (A_1) with an increase in relative percentage of the intermediate 380 ps lifetime component (A_2) in the 650–680 nm excitation region. Also shown in Fig. 2 is the excitation spectrum for fluorescence collected with a 680 nm interference filter. The weight of the short component is systematically lower and the weight of the intermediate component systematically higher than at 715 nm. We also observed a similar emission wavelength effect at excitation wavelengths greater than 680 nm. A_1 increases at the expense of A_2 as the collected emission wavelength is increased from 700 to 730 nm.

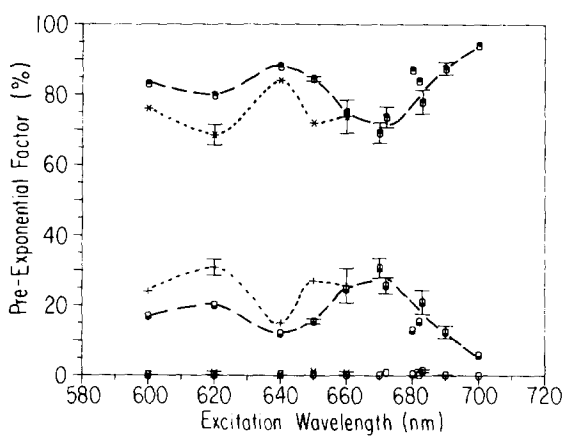

Fig. 2. Excitation wavelength study of dark-adapted barley chloroplast fluorescence decays. The relative percentage of each pre exponential factor is shown vs. excitation wavelength. The dashed lines correspond to fluorescence wavelengths greater than 710 nm, $A_1(\bullet)$, $A_2(\bullet)$, $A_3(0)$. The dotted lines correspond to fluorescence wavelengths collected at 680 ± 5 nm, $A_1(*)$, $A_2(+)$, $A_3(\times)$. A_1, A_2 and A_3 correspond to the preexponential factors of the short (112 ps), intermediate (380 ps), and long (2214 ps) lifetime components, respectively, in the fluorescence decay. Typical error bars are shown.

TABLE I

AVERAGE PARAMETERS OF TRIPLE-EXPONENTIAL FIT OF BARLEY AND SPINACH CHLOROPLAST FLUORESCENCE DECAYS

Values in parentheses are 1 S.D. of the associated value listed above.

Chloroplast Type	No. of decays averaged	Reduced χ^2	1/e lifetimes (ps)			Preexponential factors			Relative fluorescence quantum yield			Absolute quantum yield
			T_1	T_2	T_3	A_1	A_2	A_3	ϕ_1	ϕ_2	ϕ_3	
Barley, [a]	74	1.20	112	380	2214	0.788	.207	0.007	0.48	0.43	0.08	0.011
flowed		(0.37)	(33)	(100)	(658)	(0.074)	(0.071)	(0.010)	(0.20)	(0.22)	(0.12)	(0.003)
Barley, [b]	22	1.25	134	675	2131	0.688	0.254	0.059	0.24	0.44	0.32	0.023
unflowed		(0.25)	(51)	(238)	(908)	(0.141)	(0.111)	(0.051)	(0.14)	(0.31)	(0.34)	(0.009)
Spinach, [c]	6	1.14	87	318	2312	0.623	0.374	0.002	0.30	0.67	0.03	0.010
flowed		(0.13)	(38)	(37)	(328)	(0.074)	(0.077)	(0.003)	(0.15)	(0.21)	(0.04)	(0.002)
Spinach, [d]												
unflowed	1	1.09	75	595	1593	0.52	0.38	0.10	0.09	0.54	0.37	0.024

[a] Parameters of triple-exponential fit of dark-adapted barley chloroplast fluorescence decay. Average of 74 decays excited from 600 to 700 nm, with collected emission wavelengths ranging from 665 to 730 nm. Sample flow rate is 1 l/min.

[b] Same as a except samples were not flowed (constantly illuminated) and 22 samples were averaged.

[c] Parameters of triple-exponential fit of dark-adapted spinach fluorescence decays.

[d] Same as c except the sample was not flowed.

Unflowed barley chloroplasts were excited at wavelengths from 600 to 700 nm and fluorescence was collected at various wavelengths. Unflowed chloroplasts absorb photons continuously at a rate of approx. 0.1–2.0 photons/reaction center per ms. Table I lists the average parameters of a triple-exponential fit to 22 data files and Fig. 3 shows a typical fitted decay curve. The unflowed barley chloroplasts show a 2-fold increase in fluorescence quantum yield, 0.023 compared to 0.011 for dark-adapted (flowed) barley chloroplasts. The intermediate lifetime increases to 600–800 ps in unflowed samples compared to 380 ps for flowed samples. In addition, the long-lifetime component weight (A_3) increases markedly from 0.007 to 0.059. The excitation wavelength plot for the unflowed barley chloroplast is not complete, however, an emission wavelength effect is discernible at 620, 640 and 650 nm, similar to that in flowed samples.

The fluorescence decays of spinach chloroplasts have been measured (see Table I) and are qualitatively similar to the barley decays. The A_1 are lower and A_2 higher for dark-adapted spinach than for barley. Haehnel et al. [15] have measured similar values for the spinach decays. Once again we see the characteristic 2-fold increase in absolute quantum yield for unflowed (preilluminated) samples, where T_2 and A_3 increase.

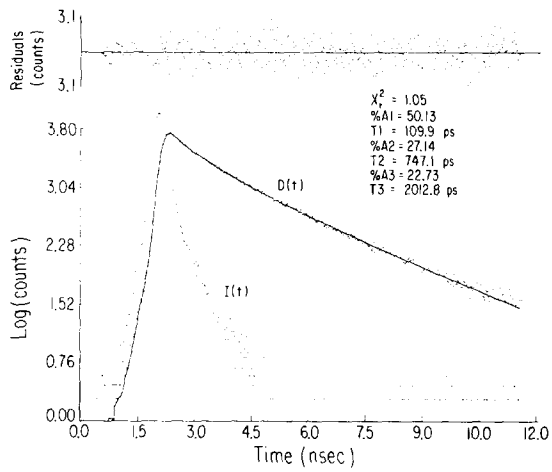

Fig. 3. Fluorescence decay of unflowed barley chloroplasts with approx. 0.3 photons/reaction center per ms of 600 ± 1 nm light absorbed by the sample. The collected emission wavelength is 680 ± 10 nm. The curve and points labelled $D(t)$ are a triple-exponential fit (curve) to the measured decay (points) using the peak (points) labelled $I(t)$ to deconvolute. The residuals for the fit are shown above.

The effect of the laser pulse repetition rate and intensity on the flowed barley chloroplast fluores-

TABLE II

COMPARISON OF CALCULATED INCIDENT LIGHT INTENSITIES AND PROBABILITIES OF MULTIPLE HITS FOR PULSE SELECTION vs. REVERSE CONFIGURATION SINGLE-PHOTON-COUNTING TECHNIQUES

Experimental single-photon-counting technique	Single pulse intensity [a] (photons/cm^2 per pulse	Photons absorbed [b]/ reaction center [c] per pulse	Probability of multiple hits/ reaction center per pulse	Average probability [d] of preillumination/ reaction center
Pulse selection with two Pockels cells in series	$3.9 \cdot 10^{11}$	$1.9 \cdot 10^{-3}$	$1.8 \cdot 10^{-6}$	0.02
Pulse selection with one Pockels cell	$4.9 \cdot 10^{11}$	$2.4 \cdot 10^{-3}$	$2.9 \cdot 10^{-6}$	0.28
Reverse configuration	$6.1 \cdot 10^{8}$	$3.2 \cdot 10^{-6}$	$6.0 \cdot 10^{-12}$	0.02

[a] These calculations assume 150 mW of 600 nm excitation is incident on a 0.06 cm diameter beam spot at a rate of 45.656 kHz when selecting or 91.312 MHz for the reverse counting configuration. The loss of light through each Pockels cell is 50% and the efficiency of pulse selection is assumed to be 0.8. Experiments with one Pockels cell usually employ a 50% transmitting neutral density filter in the excitation beam, and the reverse counting experiments had three 10% transmitting neutral density filters in addition, to reduce incident light levels.

[b] The chloroplast sample contains 3 mg total Chl/l and has an absorbance of 0.017 (corrected for scattered light) at 600 nm.

[c] The reaction center is assumed to have 250 Chl associated with it as a light-harvesting antenna.

[d] The average probability of preillumination is the calculated probability of two or more photons being absorbed in half the transit time of the chloroplasts through the beam spot. The transit time is 0.94 ± 0.47 ms.

cence decays has been investigated. Table II shows the results of a sample calculation of incident light intensity for three different experimental arrangements with 600 nm excitation. (Note that all intensity and probability values in Table II are upper limits.) The use of two Pockels cells in series for pulse selection, which reduced the cumulative intensity between selected excitation pulses, gave identical experimental decays to that obtained using a single Pockels cell throughout the entire excitation and emission wavelength region studied. This makes us confident that our dark-adapted results were not distorted by preillumination. The calculated quantum yield of fluorescence of barley chloroplasts, 0.011 ($\pm$0.003) (see Table I), and spinach chloroplasts, 0.010 ($\pm$0.002), compare well with steady-state value of 0.007 by Boardman et al. [30] for spinach chloroplasts, whereas values obtained by Searle et al. [1] of 0.015 for barley chloroplasts and Haehnel et al. (calculated from lifetimes in Ref. 15) for spinach chloroplasts of 0.0153 are somewhat higher. Reverse time-to-amplitude converter configuration experiments which employ lower single-pulse intensities (see Table II) gave identical experimental decays to those obtained with one or two Pockels cells at 600 nm. Table II shows that the probability of multiple hits and hence exciton annihilation was negligible. In addition, our single-pulse intensities were between 10^8 and 10^{12} photons cm^2 per pulse whereas the threshold for exciton annihilation has been previously reported to be at 10^{13}–10^{14} photons/cm^2 per pulse [23–25].

Discussion

The object of this paper has been to measure the fluorescence decay kinetics of dark-adapted chloroplasts and to determine what these decays mean in terms of the structural organization of the photosynthetic light-harvesting system. We have determined the fluorescence decay kinetics of barley chloroplasts and performed an excitation wavelength study which introduces an important new aspect to the discussion of the decay components in terms of phenomenological excitation-transfer paths and photochemical trapping.

Shipman [31] has presented a theoretical model of the excitation transfer and quenching for a simple photosynthetic unit composed of a reaction center and associated core of antenna chlorophylls. A single-exponential decay (except at times less than 15 ps) of excited chlorophyll molecules is obtained with lifetimes ranging from 10 to 250 ps, depending on the specifics of the calculation. The calculated lifetime is a function of the chorophyll concentration, R_0 parameter for Förster transfer, detrapping rate, and randomly generated chlorophyll position and orientations. A lifetime of 55 ps obtained in these model calculations for a P-700 trap surrounded by antenna chlorophylls (with maximum absorbance at 678 nm), agrees quite well with the experimental value (112 ps [12], $<$ 70 ps [9]) measured for larger PS I digitonin particles, containing about 200 Chl per reaction center. Preliminary studies of a more enriched PS I preparation, the P-700 Chl *a* protein (40–60 Chl *a* per PS I reaction center with no Chl *b*) isolated by hydroxyapatite chromatography of Triton X-100-solubilized membranes [32], gave premarily a 30–50 ps single-exponential decay. Kamogawa et al. [33] show a 25 ps rise time for the 700 nm absorbance of open P-700 in highly enriched particles (8–10 Chl per P-700) under single-photon excitation.

Application of Shipman's results from a reaction center and homogeneous antenna array to the more complex situation found in chloroplasts without a similar, but more formidable, calculation must be treated with caution. In particular, attempts to assign the different exponential decay components measured to certain collections of emitters such as PS I, PS II, the Chl *a*/*b* protein and combinations thereof, and to specific excitation-transfer paths may not be valid in a system where the excitation lifetime is not simply controlled by diffusion to an irreversible trap and where spillover can be large.

As a preliminary to a more detailed calculation, it is possible to present a qualitative discussion of the relationship between the measured fluorescence decays and the organization and energy-transfer paths in the light-harvesting array of chloroplasts. Consider as a model an isolated photosynthetic unit containing a PS I and PS II reaction center. There are two ways of assigning different lifetimes to particular reaction centers; (i) each reaction center has a distinct trapping probability,

is located in a homogenous antenna, and is far enough away from the other reaction center for low spillover; or (ii) each reaction center has equal trapping probability, but different migration kinetics in its antenna. The different migration kinetics may arise from different antenna pigment coupling in PS I versus PS II or from different array sizes. For example, if the PS II antenna contains most of the Chl *a/b* protein, in addition to core light-harvesting Chl *a*, this will lead to different migration times and hence lifetimes. For the two cases above, a biexponential decay of the chlorophyll population is expected. In the following we propose two models. The first model utilizes the simplest possible assumption that one decay component belongs to PS I and the other to PS II. Applying this model to our data for dark-adapted barley chloroplasts, fluorescence originating from excited chlorophyll transferring energy to PS I is associated with the 112 ps lifetime component, and fluorescence originating from pigments transferring energy to PS II is assigned to the 380 ps lifetime component of the decay. The 2214 ps lifetime component of the fluorescence, which may originate from nonphotochemical trapping in the outer antenna (e.g., fluorescence originating from decoupled Chl *a/b* proteins [34]), an effect of closed traps (e.g., charge recombination [15]), or quenching by chlorophyll or carotenoid triplets, will be neglected in this discussion as it is a minor component for dark-adapted chloroplasts. Experimental support for the above assignment comes from the PS I particle fluorescence lifetime determination as described above. The work of Boardman et al. [30] indicates that a $10000 \times g$ PS II digitonin particle has a fluorescence quantum yield 4-times that of the $144000 \times g$ PS I particle. This implies that the PS II particle lifetime is 4-times larger than that of the PS I particle. Searle et al. [35] measured a 500 ps lifetime for a PS II particle isolated similarly, however, the photochemical state of the PS II digitonin particles is not known. The excitation wavelength study (Fig. 2) shows qualitative agreement with the excitation study of Ried [36] in the 600–730 nm wavelength region, if we assign the 112 ps lifetime component to energy transfer resulting in PS I action and the intermediate 380 ps lifetime to energy transfer resulting in PS II action. Comparison of the deviation of either $\%A_1$ or $\%A_2$ about the average value (see Fig. 2) to the difference between PS I and PS II action measured by Ried as a function of excitation wavelength (see Fig. 6 in Ref. 36) shows qualitative agreement in the 640–730 nm region. Assignment of the short (112 ps) lifetime to PS I is also favored by qualitative ideas about detrapping. Detrapping is expected to be larger for PS II than PS I, simply because P-680 is nearer in absorbance wavelength to the bulk antenna pigments than P-700, making PS I detrapping less energetically favorable [31].

The major drawback of this model is that our data indicate that 79% of the initial absorbed excitation is quenched by PS I. This would require either (i) 4-times as many PS I reaction centers as PS II reaction centers independent of the connectivity of their antenna arrays or (ii) unconnected PS I and PS II reaction center antenna arrays where the antenna array of PS I reaction centers has a 4-times higher absorbance cross-section (larger antenna array). These requirements are not supported by previous work indicating that the numbers of PS I and PS II reaction centers in mature barley chloroplasts are approximately equal (Alberte, R.S., unpublished results).

Measurements of the distribution of pigments associated with PS I and PS II reaction centers, and the Chl *a/b* protein [37] also do not support this model. The Chl *a/b* protein represents 50–60% of the total chlorophyll and is believed to transfer energy prediminately to the PS II reaction center. Hence, for equal numbers of PS I and PS II with similar core array sizes we would expect $A_1 \cong 0.25$ and $A_2 \cong 0.75$. However, chemical factors such as the phosphorylation of the Chl *a/b* protein, or agents which influence chlorophyll-chlorophyll coupling both intra- and inter protein, may effect the inter photosystem excitation-energy distribution.

A second model of an isolated photosynthetic unit which may be applicable to dark-adapted chloroplasts is to assume that the 112 ps lifetime component respresents the decay of excited antenna chlorophylls which are quenched by or closely associated with either PS I or efficiently quenching PS II reaction centers. The intermediate 380 ps lifetime component represents either (i) the decay of excited antenna quenched by a PS II

reaction center which quenches less efficiently or (ii) the transfer of excitation from less efficiently coupled antenna pigments in the Chl *a/b* protein. The excitation study (Fig. 2) does not exclude this model. There is a decrease in A_1 with increased A_2 in the 650–680 nm wavelength region; this region favors absorbance by chlorophyll in the Chl *a/b* protein [39]. This also supports case ii of the first model if the Chl *a/b* protein acts merely as a larger antenna for PS II. Haehnel et al. [15] have measured the fluorescence properties of intermittent light grown pea chloroplasts depleted of Chl *a/b* protein and found that the decays are similar to those of normal pea chloroplasts, i.e., there is still an intermediate lifetime component. This result makes the migration-limited kinetics of our second model (case ii) unlikely. In addition, Shuvalov et al. [40] have published preliminary results on the fluorescence decay kinetics of enriched PS II particles containing no Chl *a/b* protein [41] and found that the fluorescence lifetime varies with overall sample redox potential and preillumination history. Hence, the assignment of the 100 and 400 ps lifetimes as in our second model (case i) to PS II in different photochemical redox states is reasonable.

Concluding Remarks

We have discussed simple photosynthetic unit light-harvesting array models which may describe the dark-adapted barley chloroplast fluorescence decay kinetics. The models illustrate the complexity and assumptions necessary in studying excitation dynamics in the chloroplast. Our data support a photosynthetic unit model in which 70–90% of the photons absorbed are quenched by either PS I or efficiently quenching PS II in a process where the fluorescence lifetime is 100 ps. The origin of the intermediate 380 ps component is probably due to excitation transfer to a PS II reaction center in a redox state which quenches less efficiently. The excitation wavelength study (Fig. 2) supports this assignment as the Chl *a/b* protein is believed to transfer energy predominately to PS II and we see an increase in the magnitude of A_2 where the Chl *a/b* protein absorbance is higher.

Acknowledgements

We would like to thank Alan Friedman for many helpful discussions of photosynthesis, Albert Cross, who is responsible for the plotting routines, and Dr. Daniel McDonald for technical assistance. We also thank Professor Kenneth Sauer for sending us a preprint of his work prior to publication. R.S.A. was an Andrew Mellon Fellow and G.R.F. was an Alfred P. Sloan Foundation Fellow during a portion of this research. This work was supported by a grant from the Research Corporation to G.R.F. and NIH GM-23944 and NSF PCM 78-10535 to R.S.A. Acknowledgement is made to the donors of the Petroleum Research Fund administered by the American Chemical Society for partial support of this research.

References

1 Searle, G.F.W., Tredwell, C.J., Barber, J. and Porter, G. (1979) Biochim. Biophys. Acta 545, 496–507
2 Barber, J., Searle, G.F.W. and Tredwell, C.J. (1978) Biochim. Biophys. Acta 501, 174–182
3 Campillo, A.J., Shapiro, S.L., Geacintov, N.E. and Swenberg, C.E. (1977) FEBS Lett. 83, 316
4 Geacintov, N.E., Breton, J., Swenberg, C.E., Campillo, A.J., Hyer, R.C. and Shapiro, S.L. (1977) Biochim. Biophys. Acta 461, 306–312
5 Yu, W., Pelligrino, F. and Alfano, R.R. (1977) Biochim. Biophys. Acta 460, 171–181
6 Paschenko, V.Z., Protasov, S.P., Rubin, A.B., Timofeev, K.N., Zamazova, L.M. and Rubin, L.B. (1975) Biochim. Biophys. Acta 408, 143–153
7 Porter, G., Synowiec, J.A. and Tredwell, C.J. (1977) Biochim. Biophys. Acta 459, 329–336
8 Beddard, G.S. and Porter, G. (1977) Biochim. Biophys. Acta 462, 63–72
9 Borisov, A. Yu. and Il'ina, M.D. (1969) Mol. Biol. 3, 391–405
10 Borisov, A. Yu. and Il'ina, M.D. (1973) Biochim. Biophys. Acta 305, 364–371
11 Jameson, D.M. and Weber, G. (1981) J. Phys. Chem. 85, 953–958
12 Beddard, G.S., Fleming, G.R., Porter, G., Searle, G.F.W. and Synowiec, J.A. (1979) Biochim. Biophys. Acta 545, 165–174
13 Sauer, K. and Brewington, G.T. (1978) in Proceedings of the 4th International Congress on Photosynthesis (Hall, D.O., Coombs, J. and Goodwin, T.W., eds.), pp. 409–421, The Biochemical Society, London
14 Sauer, K. (1981) in Proceedings of the 5th International Congress on Photosynthesis (Akoyunoglou, G., ed.), Vol., pp. 000–000, Balaban International Science Services, Philadelphia

15 Haehnel, W., Nairn, J.A., Reisberg, P. and Sauer, K. (1982) Biochim. Biophys. Acta 680, 161–173
16 Mills, W.R. and Joy, K.W. (1980) Planta 148, 75–83
17 Cockburn, W., Walker, D.A. and Baldry, C.W. (1968) Biochem. J. 197, 89
18 Avron, M., Jagendorf, A.T. and Evans, M. (1957) Biochim. Biophys. Acta 26, 262–269
19 Hall, D.O. (1972) Nat. New Biology 235, 125–126
20 Delieu, T. and Walker, D.A. (1972) New Phytol. 71, 201–225
21 McC. Lilley, R., Fitzgerald, M.P., Rienits, K.G. and Walker, D.O. (1975) New Phytol. 75, 1–10
22 Marason, E.G. (1981) Opt. Commun. 37, 56–58
23 Porter, G., Synowiec, J.A. and Tredwell, C.J. (1977) Biochim. Biophys. Acta 459, 329–336
24 Beddard, G.S. and Porter, G. (1977) Biochim. Biophys. Acta 462, 63–72
25 Campillo, A.J., Shapiro, S.L., Kollman, V.H., Winn, K.R. and Hyer, R.C. (1976) Biophys. J. 16, 93–97
26 Cramer, L.E. and Spears, K.G. (1978) J. Am. Chem. soc. 100, 221–227
27 Bevington, P.R. (1969) Data Reduction and Error Analysis for the Physical Sciences, p. 89, McGraw-Hill, New York
28 Knight, A.E.W. and Selinger, B.K. (1971) Spectrochim. Acta 27A, 1223–1234
29 Grinvald, A. and Steinberg, I.Z. (1974) Anal. Biochem. 59, 583–598
30 Boardman, N.K., Thorne, S.W. and Anderson, J.M. (1966) Proc. Natl. Acad. Sci. U.S.A. 56, 586–593
31 Shipman, L.L. (1980) Photochem. Photobiol. 31, 157–167
32 Shiozawa, J.A., Alberte, R.S. and Thornber, J.P. (1974) Arch. Biochem. Biophys. 165, 388–397
33 Kamogawa, K., Namiki, A., Nakashima, N., Yoshihara, K. and Ikegami, I. (1981) Photochem. Photobiol. 34, 511–516
34 Lotshaw, W.T., Alberte, R.S. and Fleming, G.R. (1982) Biochim. Biophys. Acta 682, 75–85
35 Searle, G.F.W., Barber, J., Harris, L., Porter, G. and Tredwell, C.J. (1977) Biochim. Biophys. Acta 459, 390–401
36 Ried, A. (1972) in Proceedings of the 2nd Congress on Photosynthesis (Forti, G., Avron, M. and Melandri, A., eds.), pp. 763–772, Junk, The Hague
37 Thornber, J.P., Alberte, R.S., Hunter, F.A., Shiozawa, J.A. and Kan, K.-S. (1978) Brookhaven Symp. Biol. 28, 132–148
38 Allen, J.F., Bennet, J., Steinbeck, K.E. and Arntzen, C.J. (1981) Nature 291, 25–29
39 Brown, J.S., Alberte, R.S. and Thornber, J.P. (1974) in Proceedings of the 3rd International Congress on Photosynthesis (Avron, M., ed.), pp. 1951–1962, Elsevier, Amsterdam
40 Shuvalov, V.A., Klimov, V.V., Dolan, E., Parson, W.W. and Ke, B. (1980) FEBS Lett. 118, 279–282
41 Ke, B., Sahu, S., Shaw, E.R. and Beinert, H. (1974) Biochim. Biophys. Acta 347, 36–48